Editing the immunopeptidome of melanoma cells using a potent inhibitor of endoplasmic reticulum aminopeptidase 1 (ERAP1)

Despoina Koumantou, Eilon Barnea, Adrian Martin-Esteban, Zachary Maben, Athanasios Papakyriakou, Anastasia Mpakali, et al.

Cancer Immunology, Immunotherapy

ISSN 0340-7004
Volume 68
Number 8

Cancer Immunol Immunother (2019)
68:1245-1261
DOI 10.1007/s00262-019-02358-0

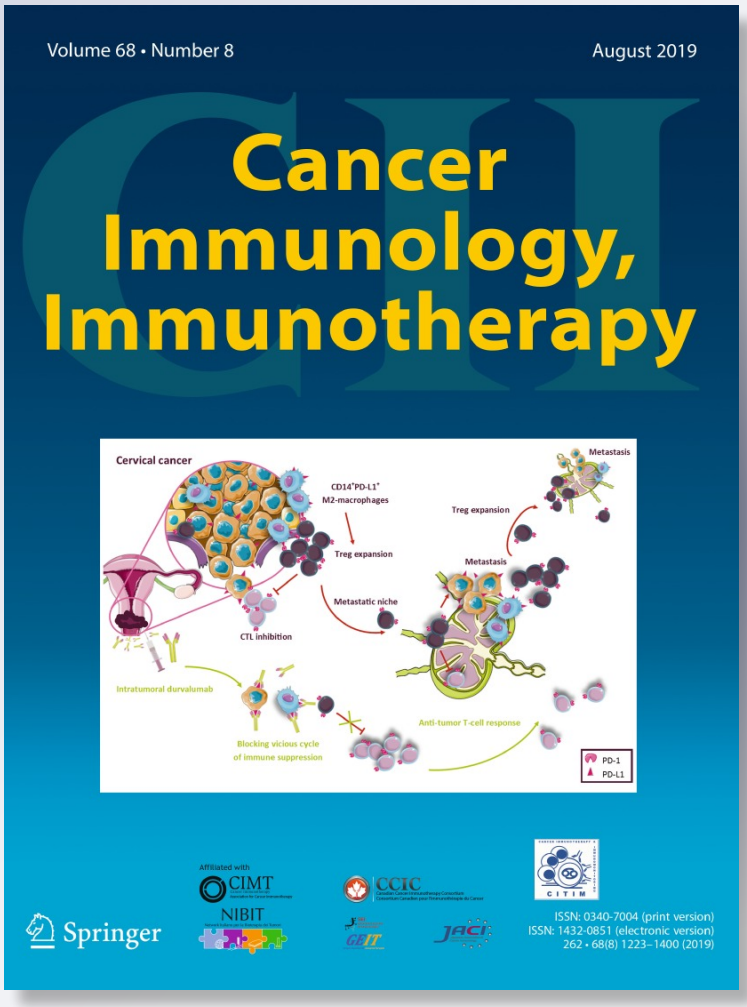

Springer

Cancer Immunology, Immunotherapy (2019) 68:1245–1261
https://doi.org/10.1007/s00262-019-02358-0

ORIGINAL ARTICLE

Editing the immunopeptidome of melanoma cells using a potent inhibitor of endoplasmic reticulum aminopeptidase 1 (ERAP1)

Despoina Koumantou[1] · Eilon Barnea[2] · Adrian Martin-Esteban[3] · Zachary Maben[4] · Athanasios Papakyriakou[1] · Anastasia Mpakali[1] · Paraskevi Kokkala[5] · Harris Pratsinis[1] · Dimitris Georgiadis[5] · Lawrence J. Stern[4] · Arie Admon[2] · Efstratios Stratikos[1]

Received: 10 December 2018 / Accepted: 11 June 2019 / Published online: 20 June 2019

Abstract

The efficacy of cancer immunotherapy, including treatment with immune-checkpoint inhibitors, often is limited by ineffective presentation of antigenic peptides that elicit T-cell-mediated anti-tumor cytotoxic responses. Manipulation of antigen presentation pathways is an emerging approach for enhancing the immunogenicity of tumors in immunotherapy settings. ER aminopeptidase 1 (ERAP1) is an intracellular enzyme that trims peptides as part of the system that generates peptides for binding to MHC class I molecules (MHC-I). We hypothesized that pharmacological inhibition of ERAP1 in cells could regulate the cellular immunopeptidome. To test this hypothesis, we treated A375 melanoma cells with a recently developed potent ERAP1 inhibitor and analyzed the presented MHC-I peptide repertoire by isolating MHC-I, eluting bound peptides, and identifying them using capillary chromatography and tandem mass spectrometry (LC-MS/MS). Although the inhibitor did not reduce cell-surface MHC-I expression, it induced qualitative and quantitative changes in the presented peptidomes. Specifically, inhibitor treatment altered presentation of about half of the total 3204 identified peptides, including about one third of the peptides predicted to bind tightly to MHC-I. Inhibitor treatment altered the length distribution of eluted peptides without change in the basic binding motifs. Surprisingly, inhibitor treatment enhanced the average predicted MHC-I binding affinity, by reducing presentation of sub-optimal long peptides and increasing presentation of many high-affinity 9–12mers, suggesting that baseline ERAP1 activity in this cell line is destructive for many potential epitopes. Our results suggest that chemical inhibition of ERAP1 may be a viable approach for manipulating the immunopeptidome of cancer.

Keywords Inhibitor · Aminopeptidase · MHC · Proteomics · Melanoma · Enzyme

Electronic supplementary material The online version of this article (https://doi.org/10.1007/s00262-019-02358-0) contains supplementary material, which is available to authorized users.

✉ Efstratios Stratikos
stratos@rrp.demokritos.gr; stratikos@gmail.com

[1] National Centre for Scientific Research Demokritos, Patriarchou Gregoriou and Neapoleos 27, Agia Paraskevi, 15341 Athens, Greece

[2] Faculty of Biology, Technion - Israel Institute of Technology, Haifa, Israel

[3] Centro de Biologia Molecular Severo Ochoa (Consejo Superior de Investigaciones Cientificas, Universidad Autonoma), Madrid, Spain

[4] Department of Pathology, University of Massachusetts Medical School, Worcester, MA, USA

[5] Laboratory of Organic Chemistry, Department of Chemistry, National and Kapodistrian University of Athens, Athens, Greece

Abbreviations

ARTS-1	Aminopeptidase regulator of TNFR1 shedding
ATCC	American Type Culture Collection
BCA	Bicinchoninic acid
Cas9	CRISPR-associated protein 9
CRISPR	Clustered regularly interspaced short palindromic repeats
EMBL	European Molecular Biology Laboratory
ERAP1	Endoplasmic reticulum aminopeptidase 1
ERAP2	Endoplasmic reticulum aminopeptidase 2
FDR	False discovery rate
GWAS	Genome-wide association study
HCMV	Human cytomegalovirus
LC-MS/MS	Tandem liquid chromatography–mass spectrometry
LC	Liquid chromatography
MHC-I	MHC class I molecules

MS	Mass spectrometry
PILS	Puromycin-insensitive leucine aminopeptidase
PVDF	Polyvinylidene difluoride

Introduction

Immunotherapy using immune-checkpoint inhibitors is rapidly changing the landscape of cancer treatment [1]. Despite often impressive clinical results using this approach, the therapeutic benefit appears to be limited to a subset of patients. Several ongoing research efforts aim to enhance anti-cancer immune responses by potentiating the effects of immune-checkpoint inhibitors using complementary approaches. Recent analyses have revealed that the potency of immune-checkpoint inhibitor therapies depends largely on the generation of cancer-specific antigens by cancer cells [2, 3]. Furthermore, presentation of cancer-specific antigens is a major predictor of long-term survival in cancer patients [4]. Cancer-specific antigens can be detected by cytotoxic T lymphocytes, which recognize peptidic fragments (antigenic peptides) generated by proteolytic processing of cellular proteins that are loaded onto major histocompatibility class I molecules (MHC-I) and presented on the cell surface. Cytotoxic T lymphocytes play an important role in the control and progression of cancer by mounting strong cytotoxic responses against transformed or malignant cells. During the process of cancer immunoediting [5], cancer cells undergo selection which enables them to avoid adaptive immune responses and allows them to proliferate in immune-competent hosts. Strategies used by cancer cells to evade the immune response involve modulation of key immune pathways such as the expression of cell-surface inhibitory receptors and the destruction of key antigenic peptides [6, 7]. This notion was recently strengthened by two studies demonstrating that the CD28/B7 co-stimulatory pathway, a signaling interaction that is necessary for correct antigenic peptide recognition, is critical to the efficacy of anti-PD-1 therapy [8, 9]. Furthermore, in a recent study using CRISPR–Cas9 genome editing in transplantable tumors in mice, several genes in the antigen processing and presentation pathway were shown to be able to sensitize tumors to PD-1 checkpoint blockade immunotherapy [10].

Although the generation and identification of particular cancer-specific antigenic epitopes often is the focus of cancer immunotherapy research, global "antigenic signature" shifts in cancer cells have been proposed to be a more reliable predictor of the efficacy of adaptive immune responses against cancer. In a recent study of human gastrointestinal cancers, strong immune responses against particular neoepitopes were observed despite the fact that these epitopes were not shared between patients [11]. Similarly, a recent study on metastatic melanoma showed a strong correlation between the clinical outcome of treatment with a monoclonal antibody against the immune-checkpoint receptor CTLA-4 and the mutational and neoantigen load of the cancer cells, although no recurrent cancer-specific epitopes were found amongst patients [2]. These studies suggest that the presentation of novel cancer antigens is critical for robust anti-cancer immune responses, although the particular epitopes that induce such responses may vary significantly between individuals and are difficult to predict.

Antigenic peptides presented by MHC-I are generated inside the cell by complex proteolytic pathways that often begin with the degradation of intracellular proteins by the proteasome (or immunoproteasome) and end with the trimming of excess N-terminal amino acids by aminopeptidases [12]. During the last decade, the important role of endoplasmic reticulum (ER) aminopeptidases in generating antigenic peptides for MHC-I has become clearer [13, 14]. ER aminopeptidase 1 (ERAP1) processes antigenic peptide precursors to generate mature antigenic peptides of the correct length for binding onto MHC-I (usually 8–10 amino acids long) [15, 16]. A highly homologous aminopeptidase, endoplasmic reticulum aminopeptidase 2 (ERAP2), can supplement ERAP1 activity in generating antigenic peptides, but plays a secondary accessory role [17]. In addition to its role in generating antigenic peptides, several studies have found that ERAP1 can also destroy antigenic peptides by trimming them to lengths too short to bind to MHC-I [18]. Genetic down-regulation of ERAP1 has been shown to have significant impact on both the nature of antigenic peptides presented on the cell surface and on concomitant cytotoxic responses [19–25]. To this extent, ERAP1 has been suggested to be a potent editor of both the immunopeptidome, the set of peptides presented by MHC molecules, and of the immunodominance hierarchy, the pattern of T-cell responses to these peptides [20, 26].

ERAP1 is polymorphic in the human population. Many GWAS and targeted population studies have associated coding SNPs in ERAP1 with predisposition to disease, including autoimmunity, viral infection, and cancer [27, 28]. The link to autoimmunity has been repeatedly confirmed and ERAP1 SNPs are found to be in epistasis with disease-specific HLA [29, 30]. ERAP1 SNPs have also been associated with other major human diseases, including cancer, most notably with the clinical outcome in cervical carcinoma [31]. Several in vitro and cell-based studies have validated the functional association between ERAP1 and disease, and have demonstrated that ERAP1 allelic state affects enzymatic activity and the capacity to generate and/or destroy antigenic peptides [32–34]. It is becoming established that the genetic variability in ERAP1 confers a functional range of enzymatic activities and contributes to the variability of immune responses between individuals [35]. ERAP1 expression has

been targeted by pathogens as an immune evasion measure: human cytomegalovirus produces a microRNA that down-regulates ERAP1 expression by about 50%, modulating CTL responses to infected cells by reducing the generation of ERAP1-dependent antigenic epitopes [36]. Cancerous tumours of different origins can either down-regulate or up-regulate ERAP1, presumably as part of cancer immune-editing processes [37, 38]. Interestingly, many cancers were found to up-regulate ERAP1. In model systems, ERAP1 has been shown to destroy tumour-associated antigenic peptides [22, 39], suggesting that tumour antigen destruction may constitute an immune-evading strategy for some cancers. Furthermore, down-regulation of ERAP1 activity has been shown to increase CTL and NK responses towards cancer cells, and to suppress autoimmune cytotoxic responses [21, 22, 40, 41]. In a recent CRISPR–Cas9 genome editing study, ERAP1 was one of the genes demonstrated to be able to sensitize melanoma tumors to PD-1 immunotherapy [10]. Thus, ERAP1 pharmacological inhibition in such tumours may have therapeutic value [42].

We have developed a potent ERAP1 inhibitor, DG013A, by structure-guided design based on key features of the ERAP1 active site, and shown that it can affect the presentation of specific antigens in cells and can reprogram antigen processing to elicit CTL responses against a cryptic epitope in a murine colon carcinoma model [43]. Recently, the same inhibitor has been used to down-regulate ERAP1-dependent innate immune responses such as activation of macrophage phagocytosis and NK cell activation after LPS treatment, and to suppress ERAP1-dependent Th17 responses in vitro [44, 45]. In this study, we set to examine the effects of this inhibitor on the global immunopeptidome of a melanoma cell line to test the hypothesis that ERAP1 inhibition can induce significant changes on the cellular immunopeptidome. This approach potentially could be utilized pharmacologically in the context of immunotherapy to induce robust antigenic shifts and enhance the immunogenicity of cancer cells.

Experimental methods

Cell culture

Cells were cultured in DMEM containing stable glutamine, supplemented with 10% heat-inactivated FBS (Gibco), penicillin and streptomycin and incubated at 37 °C, 5% CO_2.

Antibodies

For the immunopurification of the MHC-I molecules carrying the A375 peptidome, the W6/32 monoclonal antibody was used. The antibody was isolated from hybridoma cell culture supernatant and purified using protein G affinity chromatography. For FACS analysis, MHC-I molecules were stained with the W6/32 monoclonal antibody conjugated with FITC (Biorad, MCA81F). ERAP1 was detected in cell lysates using aminopeptidase PILS/ARTS1 antibody 6h9 (mab2334) and human aminopeptidase PILS/ARTS1 polyclonal goat IgG (R&D Systems, AF2334) as primary antibodies. ERAP2 western blots were performed using the Human ERAP2 polyclonal goat IgG (R&D Systems, AF3830). Anti-mouse IgG–HRP (HAF007) and anti-goat IgG–HRP (HAF017) were also purchased from R&D systems.

Recombinant proteins and enzymatic assays

Recombinant ERAP1 was produced from baculovirus-infected insect cells (Hi5™) as described previously [46]. Enzymatic titrations to evaluate the in vitro efficacy of the inhibitor were performed using a small fluorescent substrate assay as described previously [47].

Western blotting and genotyping

About 5×10^5 A375 cells were lysed with 500 µl lysis buffer containing 1% NP-40, 0.25% sodium deoxycholate, 1 mM EDTA, pH 8.0, complete protease inhibitors (Roche: 12326400) in 50 mM Tris–HCl, pH 7.5, and 150 mM NaCl buffer. After cell lysis, the total protein concentration was determined using bicinchoninic acid (BCA) Protein Assay Kit (Thermo Scientific, 23250). Whole cell lysates were analyzed with SDS-PAGE under reducing conditions in a 10% polyacrylamide gel. Equal amounts of total protein were loaded in each lane, based on BCA assay. The separated proteins were blotted onto a polyvinylidene difluoride (PVDF) membrane (Thermo Scientific, 88520) using the antibodies described above. Primary antibodies were used at a final concentration 2 µg/ml and the secondary antibodies were diluted 1:1000. As an HRP substrate, we used Pierce chemiluminescent western blotting substrate (Thermo scientific, 32209) and enhanced chemiluminescence was detected in LAS 4000 (Fujifilm). The images were processed using AIDA Image analyzing software. A375 cells were genotyped to determine which HLA alleles they expressed by the Center for Human Genetics and Laboratory Diagnostics, Dr. Klein, Dr. Rost and Colleagues, Ambulatory Healthcare Center, 82152 Martinsried-Germany. The anchor residues of the identified HLA molecules were determined based on the information derived from SYFPEITHI database (http://www.syfpeithi.de/) and in the case of HLA-C*16:01 from The HLA FactsBook (D. Barber, Peter Parham, and Steven Marsh).

To determine the ERAP1 SNPs carried by A375 cells, 10 million cells were washed twice with ice-cold PBS and

incubated overnight at 37 °C with lysis buffer (10 mM NaCl, 10 mM Tris–HCl pH 7.5, 10 mM EDTA, 0.5% SDS and 100 µg/ml RNAse A and 100 µg/ml proteinase K). Genomic DNA was isolated by phenol/$CHCl_3$ extraction and precipitated with 1/10 vol of 3 M sodium acetate, pH 5.2, and 2 vol of 100% ethanol. The pellet was washed with 70% ethanol, re-suspended in sterile deionized distilled H_2O and quantitated by absorbance at 260 nm. 50 ng of each DNA sample was used as template for conventional PCR. Forward and reverse primers used for exons 11, 12 and 15 are 5′-AAATGGGTG ATGTGTCTGCC-3′ and 5′-TCAAAAGCAAGGTTCCAT CC-3′, 5′-CATGATAGGTGATTTAATAACTGCTTG-3′ and 5′-TTTTCACATTCCTCCTTGAATTAAC-3′, 5′-TAC TGGTCCCTGTTTCCCTG-3′ and 5′-AAACAGAAAAGA TGCCCTTCAC-3′, respectively. The PCR products were isolated and sequenced using both the forward and reverse primers.

Synthesis of phosphinic inhibitor DG013A

The synthesis of phosphinic pseudotripeptide DG013A [43] started from the stereochemically pure building block Cbz-(*R*)-hPhe[PO(OH)CH_2](*S*)-Leu-OH (the preparation of this precursor will be reported elsewhere). Removal of the amino terminal Cbz-protecting group was performed in acidic conditions using HBr/AcOH as a deprotection medium. The hydrobromic salt of the resulting pseudodipeptide was protected with the Boc group under basic conditions using $(Boc)_2O$ as a protection reagent. This procedure afforded the building block of the formula Boc-(*R*)-hPhe[PO(OH)CH_2](*S*)-Leu-OH in 83% overall yield, starting from the Cbz-protected analog [48]. Coupling of H-(*S*)Trp-NH_2 followed a previously reported protocol which allows efficient peptide coupling in the presence of an unprotected phosphinic acid group [49]. In particular, excess of *N*-(3-dimethylaminopropyl)-*N*′-ethylcarbodiimide hydrochloride was employed as a coupling reagent, in the presence of hydroxybenzotriazole and *N*,*N*-diisopropylethylamine. Purification of the resulting Boc-protected tripeptide and subsequent standard acidic deprotection by dilute trifluoroacetic acid afforded DG013A in 75% yield for the last two synthetic steps. The compound was purified by reversed-phase HPLC on a C18 chromolith column (Merck) using a 10–50% (vol/vol) acetonitrile gradient in water containing 0.05% (vol/vol) trifluoroacetic acid. A single major peak was characterized by mass spectrometry, lyophilized, and dissolved in deionized water. The inhibitor concentration in the final working stock was calculated using the measured absorbance at 280 nm and the extinction coefficient 5700 M^{-1} cm^{-1}.

Cytotoxicity MTT assay

A375 cells (5000 cells/well) were cultured as described above in the presence of varying concentrations of DG013A (0–30 µM) for 48 h. The culture medium was replaced by 100 µl of DMEM containing 1 mg/ml MTT reagent. After incubation for another 4 h, the resultant formazan crystals were dissolved in DMSO (100 µl) and the absorbance intensity was measured on a TECAN infinite M200 microplate fluorescence reader at 540 nm with reference at 620 nm. All experiments were performed at least three times and the relative cell viability (%) was expressed as a percentage relative to untreated control cells.

A375 treatment with DG013A inhibitor

A375 cells were treated with DG013A inhibitor for a total of 6 days. The inhibitor was added to the complete culture medium at a final concentration 1 µM. The cell medium that contained the inhibitor was refreshed every 2 days. Cell cultures were incubated as usual at 37 °C, 5% CO_2. After 6 days of incubation, cells were harvested for immunopeptidome isolation or for flow cytometry. For immunopeptidome analysis, cells were cultured at a large scale and collected from flasks using accutase solution (Merck SCR005). Cell pellets were stored at − 80 °C until immunopeptidome isolation. For the flow cytometry analysis, cells were seeded in a 12-well plate and harvested with 10 mM EDTA, pH 8.0, in PBS.

Flow cytometry

Approximately 1×10^6 cells per sample were transferred in FACS tubes after harvesting, and were washed twice with 1 ml FACS buffer (1%BSA/PBS, 0.02% NaN_3). The cells were stained with 2 µl undiluted W6/32-FITC for 30 min on ice. After incubation, the cells were washed with 2 ml FACS buffer, centrifuged at 200*g* for 5 min at 4 °C and re-suspended in 300 µl FACS buffer. The samples were analyzed in a FACScalibur flow cytometer using the BD CellQuest™ Pro software. Approximately 20,000 events per sample were measured.

Preparation of immunoaffinity columns

W6/32 antibody (2 mg per column) was dialyzed in coupling buffer ($NaHCO_3$ 0.1 M, NaCl 0.5 M, pH 8.3) overnight. To generate one 1 ml bed volume of cyanogen bromide-activated Sepharose 4B (GE Healthcare 17-0430-01), 0.285 g of dry beads was used. Sepharose was rehydrated with 1 mM HCl for 30 min and then washed thoroughly with coupling buffer. The solution of the antibody was added to the beads and left for coupling overnight at 4 °C. After coupling, the beads were washed with coupling buffer and then with

blocking buffer (Tris–HCl 0.1 M, pH 8.0). After the washes the beads were transferred to a 50-ml tube with blocking buffer and were mixed for 3 h at room temperature. Finally, the beads were washed with three cycles of acidic buffer (CH_3COONa 0.1 M, NaCl 0.5 M, pH 4.0) and then basic buffer (Tris–HCl 0.1 M, NaCl 0.5 M, pH 8.0) solutions and then with 20 mM Tris–HCl, pH 7.5, 150 mM NaCl. For the pre-columns, the exact same procedure was followed with the exception of the W6/32 coupling step. The columns and the pre-columns were stored at 4 °C until needed.

Isolation of MHC-I immunopeptidome

For the isolation of the immunopeptidome, 5×10^8 cells per sample were used. Cells were lysed with 20 ml lysis buffer (Tris–HCl, pH 7.5, 150 mM NaCl, 0.5% IGEPAL CA-630, 0.25% sodium deoxycholate, 1 mM EDTA, pH 8.0, 1 × complete EDTA-free protease inhibitor cocktail tablets) for 1 h at 4 °C. The cell lysate was cleared with ultracentrifugation at 100000 g for 1 h at 4 °C and then loaded onto a cyanogen bromide-activated Sepharose pre-column, blocked as described above. The flow through from the pre-column was passed through W6/32-coupled beads three times and then washed with 20 bed volumes 20 mM Tris–HCl, pH 8.0, 150 mM NaCl, 20 bed volumes 20 mM Tris–HCl, pH 8.0, 400 mM NaCl, 20 bed volumes 20 mM Tris–HCl, pH 8.0, 150 mM NaCl and finally with 40 bed volumes 20 mM Tris–HCl, pH 8.0. The MHC-I–peptide complexes were eluted from the immunoaffinity column with 1% TFA. The peptides were separated from the MHC-I molecules using reversed-phase C18 disposable spin columns (Thermo Scientific). The fraction containing peptides was dried prior to LC-MS/MS analysis.

Mass spectrometry analysis

Each sample was analyzed in a Q-Exactive-Plus mass spectrometer (Thermo Fisher Scientific) as described previously [50]. Peptides were separated using a 7–40% acetonitrile gradient with 0.1% formic acid for 180 min and a flow rate of 0.15 l/min on a 0.075-mm × 30-cm capillary column packed with Reprosil C18-Aqua (Dr. Maisch, GmbH, Ammerbuch-Entringen, Germany). The dynamic exclusion was set to 20 s. Selected masses were fragmented from the survey scan of mass to charge ratio (m/z) 300–1800 atomic mass units at resolution of 70,000. MS/MS spectra were acquired starting at m/z 200 with a resolution of 17,500. The target value was 1×10^5, and the isolation window was 1.8 Da. Peptide sequences were assigned from the MS/MS spectra using the Max-Quant software (version 1.5.0.25) [51] and the human UniProt/Swiss-Prot database (release 2015_07: 69,693 entries). Precursor ion mass and fragment mass tolerance was set to 20 ppm, FDR was set to 0.01, peptide-spectrum matching FDR to 0.05 and oxidation (Met), acetyl (protein N terminus), and Gln to Pyro-Glu were used as variable modifications. Any identification from the reverse database and known contaminants were eliminated.

Cellular antigen processing assay

HeLa cells stably expressing H-2 Kb [18] were plated in 24-well plates and infected with recombinant vaccinia which expresses signal sequence—LEQLESIINFEKL–IRES–GFP. At the time of infection, DG013A or leucinethiol were also added to the cells. All conditions contained 0.5% DMSO. After 18–22 h, the cells were incubated with 25.D1.16 monoclonal mouse antibody, which specifically recognizes the SIINFEKL:H-2 Kb peptide MHC complex [52]. After incubating 30 min on ice, the cells were washed with Dulbecco's PBS and Alexa647-goat anti-mouse antibody was added to the cells at 1:200 (v/v) dilution. After incubating 30 min on ice, the cells were washed with Dulbecco's PBS. The cells were then re-suspended in 250 µl Dulbecco's PBS and fixed by addition of 250 µL 4% formalin in Dulbecco's PBS (v/v) for 15 min at room temperature. The fixation was stopped with the addition of 250 µl Dulbecco's PBS supplemented with 1% (v/v) fetal bovine serum and 0.01% (m/v) sodium azide. Sample GFP and Alexa 647 fluorescence was measured using a LSR-II and analyzed using the FlowJo 9.6.4 software. Singlets were identified by comparing forward scatter signal height and width, and then GFP-positive samples were identified by comparison to an uninfected control. Alexa 647 median fluorescence intensity was normalized where MFI of a sample without inhibitor treatment is set to one, and the MFI of a sample treated with 100 µM leucinethiol is set to zero. Calculation of IC_{50} was performed using Prism 6.

Results

The ERAP1 inhibitor DG013A can regulate the presentation of an ERAP1-dependent antigenic model epitope

To inhibit ERAP1 in A375 cells, we used the inhibitor DG013A, which is, to our knowledge, the most potent ERAP1 inhibitor reported to date (Fig. 1a) [43]. The inhibitor was synthesized using stereoselective synthesis as described in the experimental section and in [47]. To validate the ability of the inhibitor to inhibit ERAP1 in vitro, we performed an enzymatic titration that indicated a half-maximum inhibitory concentration of 43.5 ± 2.5 nM, which is consistent with previously published values (Fig. 1a).

To help establish a minimum dosage of the inhibitor sufficient to regulate the MHC-I presentation of

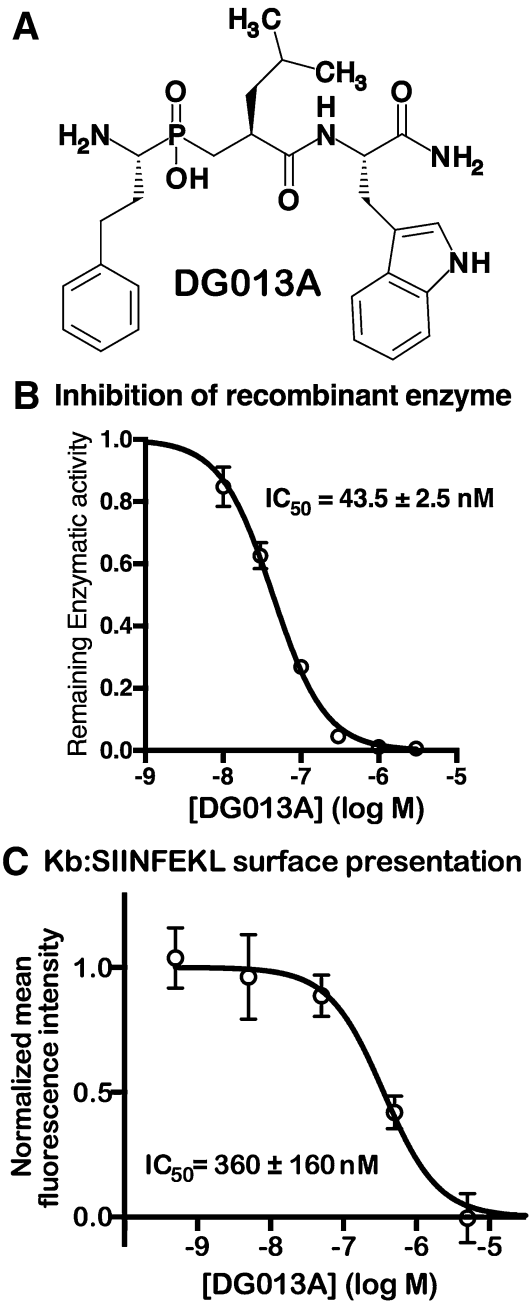

Fig. 1 Compound DG013A inhibits ERAP1 in vitro and can inhibit presentation of an ERAP1-dependent antigenic peptide by cells. **a** Chemical structure of inhibitor DG013A. **b** Titration of DG013A inhibits recombinant ERAP1 activity in vitro. **c** Titration of DG013A to HeLa:Kb cells infected with vaccinia virus that targets an N-terminally extended precursor of the SIINFEKL epitope to the ER leads to a dose-dependent reduction in surface presentation of the epitope

ERAP1-dependent epitopes, we utilized a cellular assay that follows the presentation of the ovalbumin epitope SIINFEKL, a well-characterized epitope that requires ERAP1 for presentation [18]. A HeLa cell line stably transfected to express mouse H2-K^b was infected with a vaccinia virus that targets the epitope precursor with the sequence LEQLESIINFEKL to the ER. Normally, ERAP1 processing can generate the mature epitope SIINFEKL, which when loaded onto H2-K^b is transferred to the cell surface and can be detected by a specialized monoclonal antibody [18]. Titration of increasing concentrations of DG013A resulted in a dose-dependent reduction of K^b-SIINFEKL on the cell surface with an apparent ED_{50} of 350 ± 160 nM (Fig. 1c). This finding further validated the ability of this compound to affect ERAP1-dependent antigen presentation in cells and established that using 1μM inhibitor in the cell medium should be sufficient to substantially inhibit ERAP1 in cells.

Characterization of the A375 melanoma cell line as an appropriate template to study the regulation of immunopeptidome by ERAP1

To gain insight into the effects of ERAP1 inhibition on the global immunopeptidome of human cells, we selected the A375 cell line, which has been established from malignant melanoma skin tumors. The inhibitor does not appear to be toxic to A375 cells up to a concentration of 30 μM, as judged by the MTT assay (Supplemental Figure 1). Genotyping for HLA-type revealed that A375 cells carry six MHC-I alleles, namely HLA-A*01:01:01, HLA-A*02:01:01, HLA-B*44:03:01, HLA-B*57:01:01, HLA-C*06:02:01 and HLA-C*16:01:01. Based on peptide presentation data from the SYFPEITHI database [53], we also noted the expected anchor residue positions in each allele (Supplemental Figure S2a). Using the W6/32 antibody, which can detect all human MHC class I alleles, we compared cell-surface staining on A375 cells by FACS (Supplemental Figure S2b). No significant change in MHC-I levels on the surface of A375 cells was evident when the cells were exposed to 1 μM DG013A for up to 6 days, suggesting that chemical inhibition of ERAP1 was not sufficient to produce any long-term effects on the overall MHC-I expression at the cell surface. This is consistent with a recent study that compared the effect of ERAP1 shRNA down-regulation on MHC-I surface expression in other cancer cell lines [41], and knockout of ERAP1 in transgenic HLA-B27 rats [25]. ERAP1 expression in A375 cells was validated by western blot (Supplemental Figure 2c) and found to be up-regulated by interferon-gamma, consistent with the published literature [41, 54]. We compared ERAP1 levels in the cells to the homologous ERAP2, given that DG013A also inhibits that enzyme. According to the EMBL Expression Atlas database, A375 cells express 72 transcripts per kilobase million ERAP1 RNA, but only 2 transcripts per kilobase million ERAP2 RNA [55]. Accordingly, comparing western blot signals to recombinant controls revealed that ERAP2 protein is expressed at least ten-fold less than ERAP1 (Supplemental Figure S3). Thus, we expect ERAP1 activity to be dominant compared to ERAP2

in antigen processing in A375 cells. Since ERAP1 SNPs have been shown to affect enzymatic activity and to alter the cellular immunopeptidome, we determined the ERAP1 allelic composition in A375 cells. This was done by genomic sequencing of exons 11, 12 and 15 of the ERAP1 gene since these exons harbor four common coding single nucleotide polymorphisms that have been most commonly associated with disease and functional changes [27, 28, 32]. According to sequencing results (Supplemental Figure S4), ERAP1 in A375 cells carries SNPs 528 K, 575D, 725R, 730Q, which correspond to the ancestral haplotype [56]. Interestingly, several studies have associated SNPs 528 K and 730Q with a higher enzymatic activity, suggesting that A375 cells carry a highly active ERAP1 allele [30, 32, 33].

Analysis of A375 immunopeptidome by capillary chromatography and tandem mass spectrometry

Since the inhibitor does not appear to influence cell-surface MHC-I levels but can affect the presentation of a model epitope, we set forth to evaluate its effects on the peptide repertoire presented by the natural MHC alleles in A375 cells. Towards this end, we purified MHC-I–peptide complexes from A375 cells that had been exposed to 1 μM DG013A for 6 days. A control experiment was performed in the absence of the inhibitor. A375 cells were solubilized in mild detergent and MHC-I–peptide complexes were purified by affinity chromatography using immobilized W6/32 antibody. MHC-I-bound peptides were eluted by acid extraction and analyzed by LC-MS/MS. To have sufficient statistical power to define the inhibitor-induced changes, we performed three biological replicates for each condition. A MaxQuant-style table listing all identified peptides can be freely downloaded at https://sfiler.ipta.demokritos.gr/s/qMJGBCCE6oSqi5p (password erap1a375). The cross-correlation analysis revealed good correlation between same condition replicates and a weaker correlation between cross pairs (inhibitor versus control)(Fig. 2). Both control and inhibitor samples contained many peptide sequences unique to the respective condition (Fig. 3a, boxes [a] and [b]). However, several peptides present in both conditions were detected with intensities that were statistically different (Fig. 3b). Thus, in accordance with a previous study [57], we defined peptides to be control-specific when they were either uniquely identified in the control condition or down-regulated by the inhibitor by at least fourfold (Fig. 3b, box labeled "Control"). Similarly, we defined peptides as

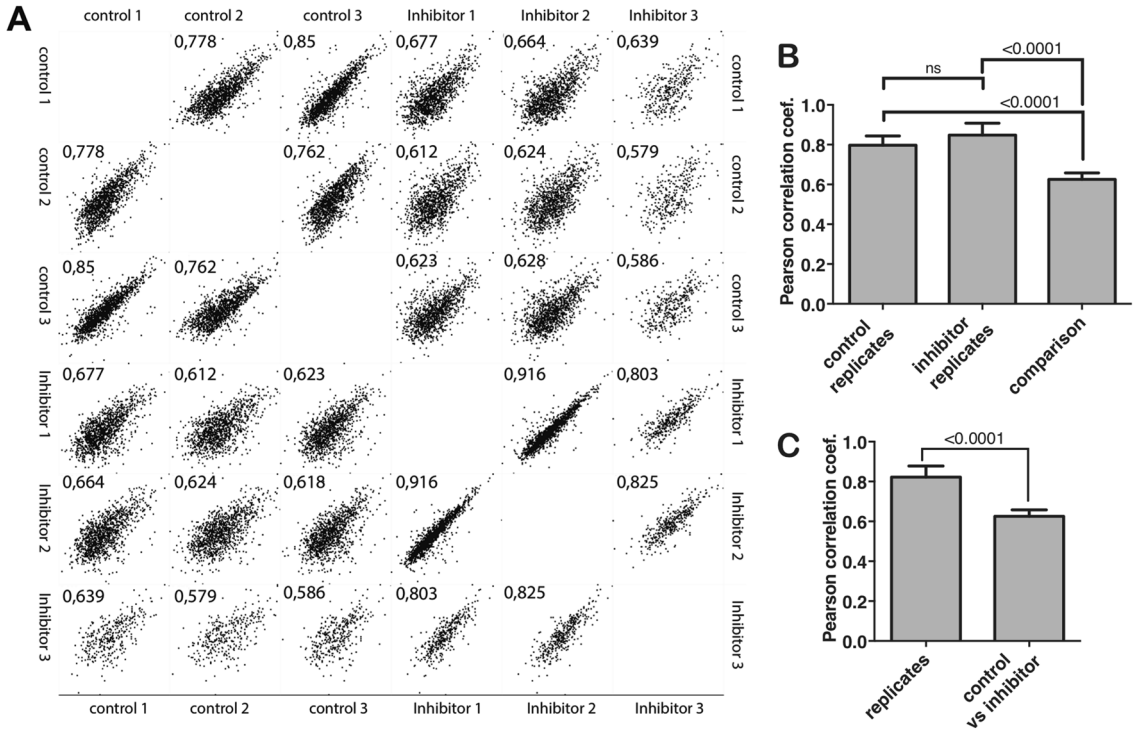

Fig. 2 Treating A375 cells with the inhibitor affects global presentation by MHC-I. **a** Correlations in peptide intensity between different experiments or replicates. The calculated Pearson coefficient is indicated in each panel. **b** Average Pearson coefficient of correlations between control replicates, inhibitor replicates, and control versus inhibitor experiments. **c** Average Pearson coefficient of correlations between replicates of the same condition and control versus inhibitor

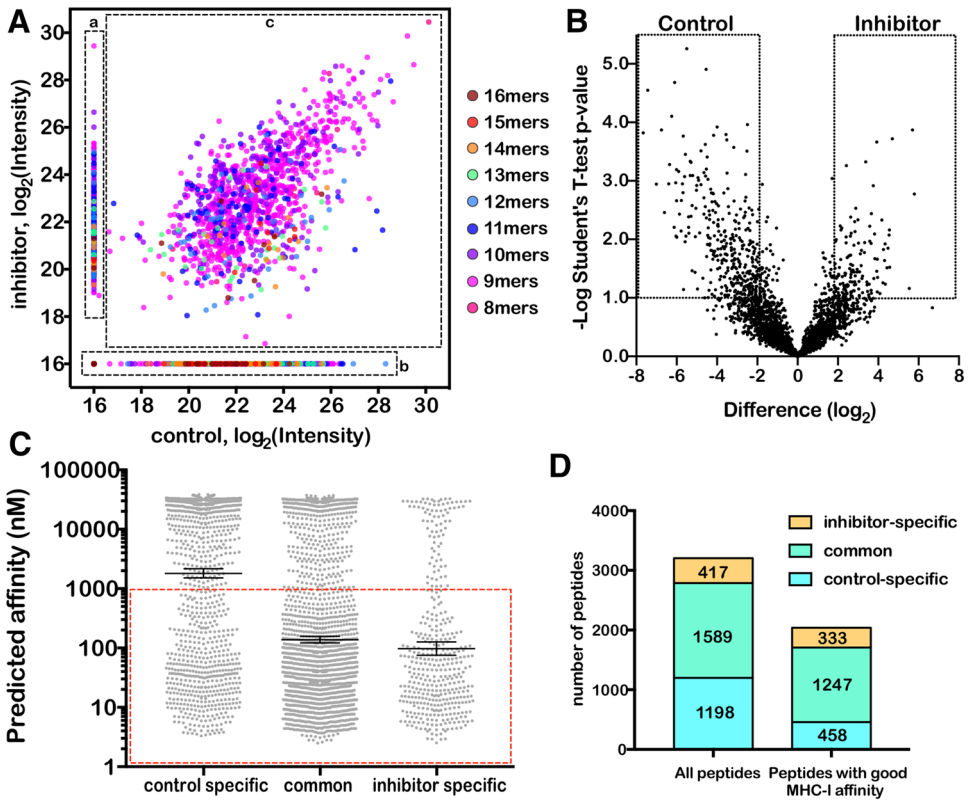

Fig. 3 Statistical analysis of inhibitor effects on presented peptides. **a** Scatter plot of the average intensities along three biological replicates of identified peptides, colored by length. Each circle corresponds to a unique peptide sequence. Peptides identified in only one condition were assigned intensities at the threshold of detection for the other condition (boxes **a**, **b**). Peptides identified in both conditions are in box **c**. Color coding indicates peptide length. **b** Volcano plot showing peptides that are either up-regulated or down-regulated by the inhibitor. Peptides within the two square areas are affected in a statistically significant manner by more than fourfold and were classified to be specific to each respective condition. **c** Predicted affinity of peptides for MHC-I alleles expressed in A375 cells, as calculated by the NetMHCcons1.1 server [60]. Affinities were calculated for each peptide for all six HLA-alleles carried by A375 cells, but only the best affinity was plotted. The boxed region indicates peptides that are predicted to bind to at least one MHC-I allele with an IC50 value below 1 μM. **d** Numbers of peptides assigned to each condition

inhibitor-specific when they were either uniquely identified in the inhibitor condition or up-regulated by the inhibitor by at least fourfold (Fig. 3b, box labeled "Inhibitor"). We defined as "common" the peptides that were common in both conditions with a less than fourfold difference in intensities between the control and inhibitor condition. Thus, we assigned 1589 peptides to be common, 1198 to be control-specific and 417 to be inhibitor-specific. Since there is an established association between affinity of a peptide ligand for MHC-I and immunogenicity [58, 59], we scored each identified peptide for predicted affinity versus the HLA alleles carried by A375 using the NetMHCcons1.1 server [60] (Fig. 3c). Based on previous studies [58, 59], 90% of all epitopes have an affinity for MHC-I below 1μM and thus we used this value as cut-off (Fig. 3c, boxed region). This analysis revealed that 38% of all identified peptides are predicted to be very weak MHC-I binders (predicted affinity > 1 μM). This set will include true MHC-I ligands with high affinity that are incorrectly predicted, true but weakly binding MHC-I ligands that are unlikely to be immunogenic, and non-binding contaminant peptides. Of the remaining 62% of peptides predicted to be good MHC-I binders, 1247 peptides were common to both conditions, 458 peptides were control-specific and 333 peptides were inhibitor-specific (Fig. 3d). To detect if any neoantigens were presented by A375 cells in our experiment, we identified 505 known coding mutations present in A375 cells and deposited in the Cancer Cell Line Encyclopedia [61], and searched for eluted peptides carrying at least one of those mutations. Only a single peptide carrying a neoantigen mutation was identified, namely peptide G**L**LPNIQAV from HIST3H2A (ENST00000366695) that carries the mutation V108L (in bold in peptide sequence), which is predicted to be a very good (8.9 nM) binder for HLA-A02:01. This single neoantigen-derived peptide, however, was present in all experiments regardless of inhibitor treatment suggesting it is not ERAP1 dependent. Overall, our results demonstrate that

incubating A375 cells with the ERAP1 inhibitor DG013A induces a significant shift in the peptides that are presented by MHC-I but this shift is limited to about one third of the cellular immunopeptidome.

Effects on presented peptide length and predicted affinity

Length is an important parameter that influences peptide binding and presentation by MHC-I, thus we analyzed the effect of the inhibitor on the length of presented peptides (Fig. 4). In all cases, most of the peptides presented were 9mers, consistent with the optimal length for MHC-I binding and with the fact that the majority of known antigenic peptides are 9mers. Amongst all peptides identified, the inhibitor-specific group had a larger percentage of 9mers compared to the control-specific group (Fig. 4a), as well as a larger percentage of 10mers and 11mers. This trend was reversed, for larger peptides, with the control group containing a larger percentage of 12–16mers. When limiting the analysis to the good MHC-I binders, the control-specific group had a very similar distribution to the common peptides, while the inhibitor-specific group had a lower percentage of 9mers and higher percentage of 10mers, 11mers and 12mers (Fig. 4b). This trend was even more apparent when we considered peptides that were detected in both conditions but were either up-regulated or down-regulated by the inhibitor (indicated in the boxed regions of Fig. 3b). For these peptides, the inhibitor reduced the percentage of 9mers from 75 to 50%, increased 10mers almost twofold, 11mers by tenfold, and 12mers by fivefold (Fig. 4c).

The inhibitor affected the average predicted affinity of the identified peptides for MHC-I. The geometric mean of the predicted affinity for the common peptides was 138 nM, whereas for the control-specific peptides 1808 nM and for the inhibitor-specific peptides 97 nM (Fig. 3c). Thus, it appears that upon inhibitor incubation, a subset of weak-binding peptides was substituted by more tightly binding peptides. This is a surprising result that suggests that ERAP1 has a strongly destructive function in this cell line. Many of the weak-binding peptides that are no longer detectable upon inhibitor incubation fall within the 12mer–16mer range. It should be noted, however, that affinity-prediction algorithms such as netMHCcons are not optimized for predicting affinity of longer peptides and thus the affinity of the 12–16mers in the control condition may be an underestimate and several good MHC-I ligands may exist in that subset [62]. Regardless, the inhibitor appears to eradicate many weakly binding 12–16mers and increase the representation of higher affinity 9–11mers.

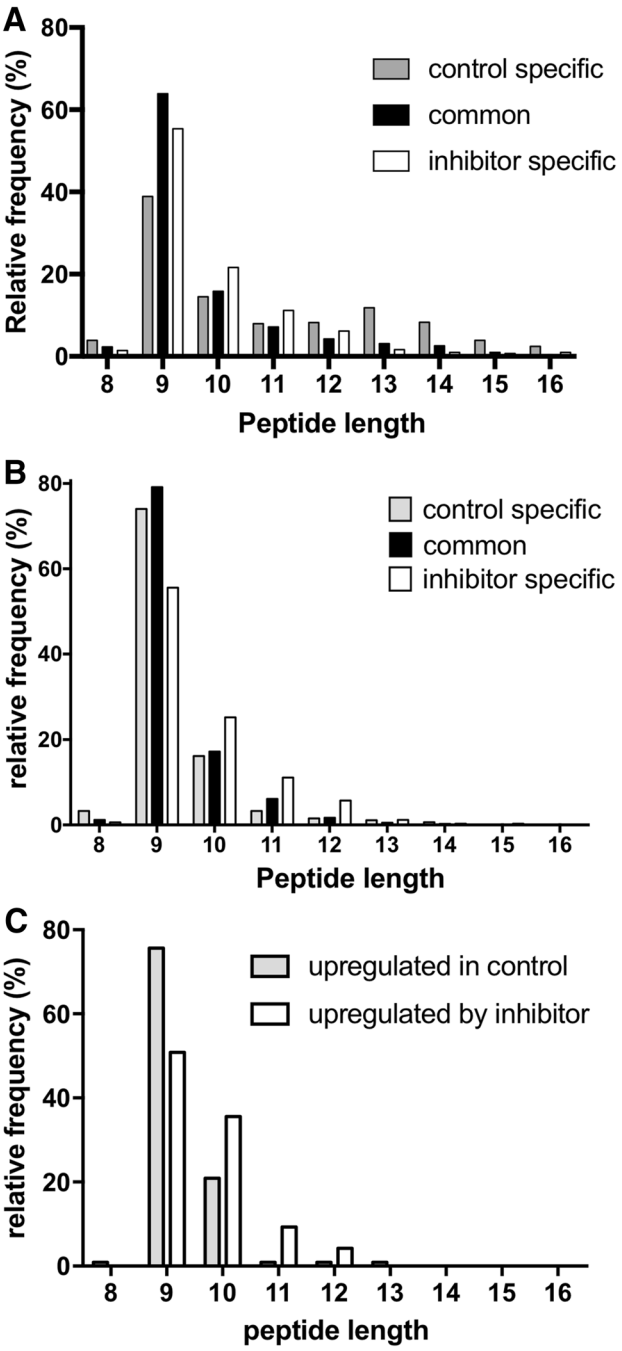

Fig. 4 The inhibitor affects the length of presented peptides. **a** Distribution of lengths of identified peptides per condition. **b** Same as in (**a**), but only for peptides predicted to bind to MHC-I with an affinity of < 1 μM. **c** Distribution of lengths of peptides that are common to both conditions but either up-regulated or down-regulated by the inhibitor for greater than fourfold (as defined in Fig. 3b)

Effects on peptide sequence

Given the enzymatic activity of ERAP1 as an aminopeptidase, we examined the effect of the inhibitors on the nature of the first amino acid of the presented peptides. It should be

noted that ERAP1 activity can in principle reduce or even eradicate the binding of peptides onto MHC-I and in this context all presented peptides carry amino acids at their N terminus that have escaped ERAP1-mediated trimming. Certain aspects of the mechanism that ERAP1 uses to trim peptides remain controversial and no consensus has been unequivocally reached on whether MHC-I binding is always protective from further trimming or can actually promote peptide degradation [63]. Analysis of the distribution of the first amino acid in the identified peptides showed that irrespective of the presence or absence of inhibitor all residues are represented, but to varying degrees (< 1 to 22%). Significant differences between the control and inhibitor conditions were evident. To visualize the changes induced by the inhibitor, we plotted the relative change of the inhibitor-specific and control-specific peptides in comparison to the common peptides since these two groups should represent groups of peptides that are either destroyed by ERAP1 or require ERAP1 for generation, respectively (Fig. 5). Overall, inhibitor treatment increased the frequency of peptides carrying on their N terminus amino acids such as Tyr, Met, Leu and Ala, previously demonstrated to be optimal substrates for ERAP1, and reduced the frequency of less optimal substrates carrying other N-terminal residues (Fig. 5a) [64]. This trend was clearer when we limited the analysis to peptides predicted to be good MHC-I binders (Fig. 5b).

Of note is the strong effect of the inhibitor on peptides that carry an N-terminal Pro residue (233 peptides), which were virtually absent from the inhibitor-treated samples (Fig. 5a). This effect was not evident when limiting the analysis to good MHC-I binders, because virtually all of the peptides starting with a Pro residue were predicted to be poor MHC-I ligands (Fig. 5b). Furthermore, this phenomenon extends to peptides with Pro at position 2 (78 peptides) and to peptides that have an Asp residue at position − 1. Since, however, the Asp–Pro bond can be self-catalytically broken during acidic treatments that are part of the isolation protocol [65], it is possible that some of the Pro-starting peptides were originally Asp–Pro in the analyzed samples. All three groups of these peptides (311 peptides in total) were over-represented in the control samples (Supplemental Figure S5a), predicted to be weak MHC-I binders (Supplemental Figure S5b), and of varied lengths (Figure S5c). Since ERAP1 cannot cleave peptides with Pro as the first or second residue [46], these peptides would be expected to be fully ERAP1 resistant and to accumulate to higher fractional levels with high ERAP1 activity. When ERAP1 is inhibited, ERAP1-sensitive peptides that are good MHC-I binders may be spared and accumulate. Such peptides can out-compete the Pro-containing peptides and reduce their relative abundance. This finding would suggest that, at least in A375 cells, ERAP1 has a strong destructive influence on many optimal MHC-I epitopes.

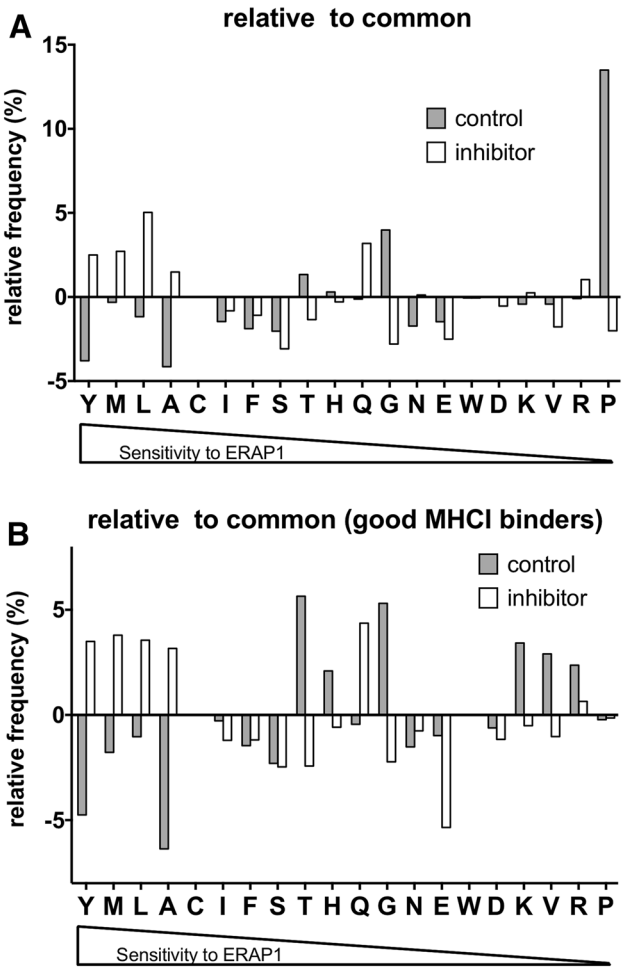

Fig. 5 Inhibitor treatment increases the abundance of peptides carrying N termini that are ERAP1 sensitive. **a** Distribution of the first amino acid of identified 9mer peptides in the control-specific and inhibitor-specific set, in comparison to the common peptides. **b** Same as in (**a**), but limited to the good MHC-I binders. Amino acids in the *x*-axis are ordered based on experimentally determined sensitivity to ERAP1 [64]

To investigate possible effects of the inhibitor on the internal sequence motifs of presented peptides, we performed Gibbs cluster analysis on the 9mer sequences of identified peptides in each set using the GibbsCluster-2.0 Server and Seq2logo servers [66, 67] (Fig. 6). This server applies the Gibbs clustering algorithm to reveal peptide sequence motifs from large groups of peptides [68]. Since we are analyzing the immunopeptidome from cells that carry six different HLA alleles that have different binding preferences (Fig. 2), clustering results will encompass binding preferences from all alleles. Figure 6 presents the clustering results for the three most dominant clusters of each set. In all cases, a minimum of two positions dominate in sequence conservation, corresponding to anchor residues preferred by respective HLA alleles. A major cluster (Fig. 6,

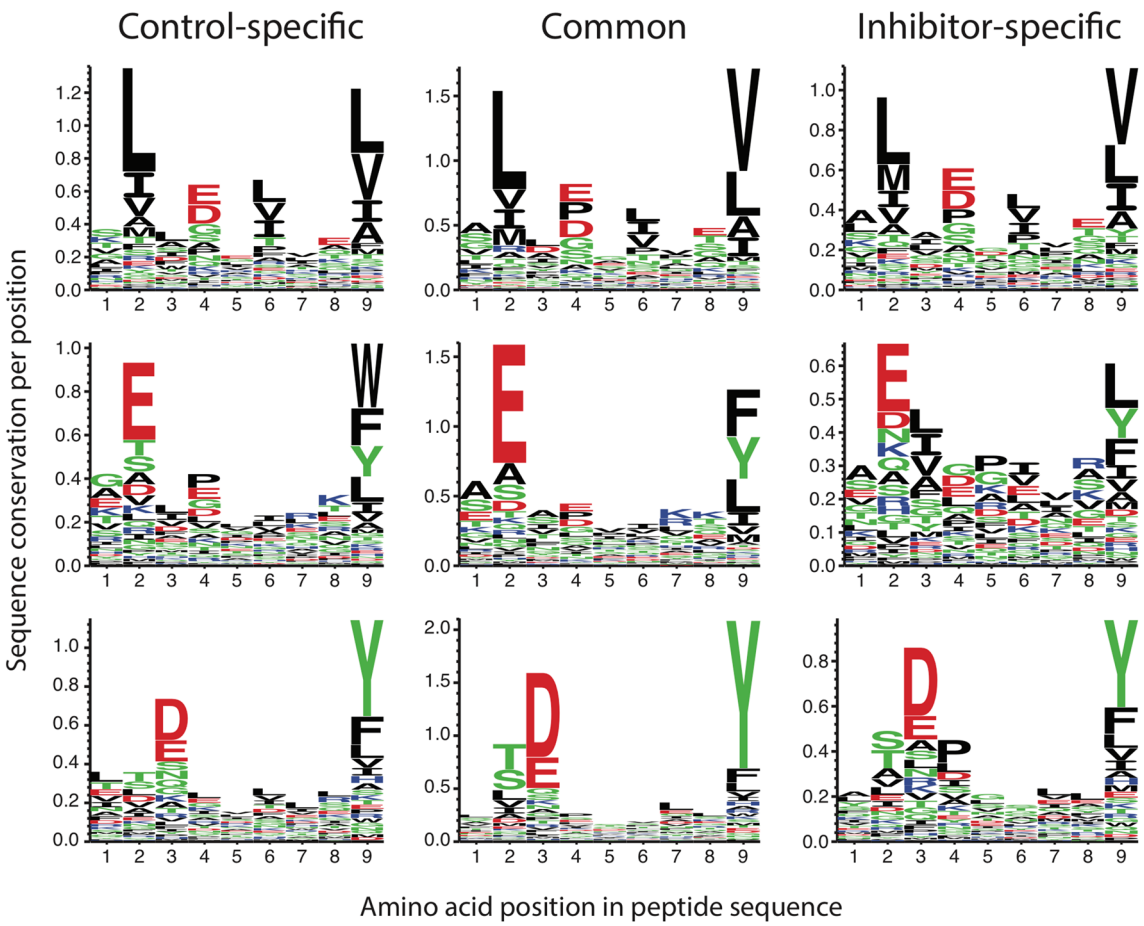

Fig. 6 Inhibitor treatment does not affect the basic sequence motifs of presented peptides. Gibbs cluster analysis of 9mer sequences of identified peptides. Analysis was performed using the GibbsCluster-2.0 Server and plotted using the Seq2logo server [66, 67]

top panels) contains peptides with hydrophobic residues at positions 2 and 9 and probably represents peptides presented by HLA-A*02:01 and to a lesser extent HLA-B*57:01 and HLA-C*16:01:01. A second major cluster (Fig. 6, middle panels) contains peptides that carry negatively charged and hydrophilic residues at position 2 and hydrophobic residues at position 9, presumably presented by HLA-B*44:03, HLA-B*57:01 and HLA-C*16:01. A third major cluster (Fig. 6, bottom panels) contains peptides with negatively charged amino acids at position 3 and hydrophobic amino acids at position 9, consistent with peptides presented by HLA-A*01:01. HLA-C*06:02 does not appear in a separate cluster possibly due to lack of a clear anchor residue in the first few positions, but is probably included in all three clusters since it prefers peptides with hydrophobic residues at position 9. Overall, the patterns revealed by cluster analysis suggest that the HLA binding preferences are dominant in selecting the majority of peptides presented, irrespective of ERAP1 activity, although ERAP1 activity can influence which peptides are presented within the constraints of the MHC-I binding preferences. Some increased heterogeneity is evident in the inhibitor-specific set, which features slightly reduced sequence conservation scores. This may be interesting immunologically in the context of the presentation of novel peptides that can induce $CD8^+$ responses, which would be increased upon ERAP1 inhibition.

Discussion

ERAP1 inhibition does not abrogate presentation and has a significant effect on the immunopeptidome

Initial studies on the effects of ERAP1 down-regulation using siRNA in HeLa cells had suggested that it can significantly impact total cell-surface MHC-I presence [18, 54, 69]. Later studies have focused more on the cargo of MHC-I and often did not show significant effects on total expression of MHC-I on the cell surface, hinting that such phenomena may be dependent on the combination of HLA alleles and cell line [25, 41, 50, 57]. In our system, we find

no evidence of significant down-regulation of cell-surface MHC-I levels by a potent ERAP1 inhibitor. This may be due to either ERAP1 not significantly affecting the levels of available peptides, or to peptide supply not being a limiting factor for MHC-I presence on the cell surface. Indeed, in a recent study, the authors demonstrated that MHC-I levels are dependent on the availability of receptive MHC-I rather than peptide supply, a mechanism that may also apply on our system [70]. Regardless of the mechanism, alteration of the MHC-I immunopeptidome without significant alteration of overall surface expression level may be highly desirable pharmacologically since down-regulation of MHC-I levels is a common immune evasion strategy by tumors [71, 72]. Our findings suggest that chemically inhibiting ERAP1 can induce significant changes in the immunopeptidome without abrogating antigen presentation.

The overall changes in the immunopeptidome induced by the ERAP1 inhibitor are modest as approximately half of the peptides presented and two-thirds of the predicted good MHC-I binders are not affected. Although this might potentially be due to incomplete inhibition of ERAP1, we think that explanation is unlikely because of the large effect observed in a cell-based presentation assay for a known ERAP1-dependent epitope, and since previous studies using transgenic animals (discussed in more detail below) also have demonstrated that a significant component of the immunopeptidome is ERAP1-independent [25, 57]. Even modest changes to the immunopeptidome, however, can result in drastic changes in cytotoxic responses by altering immunodominance [19, 20, 24]. The limited effects of ERAP1 inhibition on MHC-I expression level and modest alteration of the immunopeptidome actually may be beneficial on a therapeutic setting since this would help avoid undesirable side effects by overactivating immune responses.

The dual role of ERAP1 in generating and destroying peptides

Soon after the first discovery of ERAP1, several studies had hinted at a complex landscape regarding its effects on MHC-I-presented peptides. RNA interference of ERAP1 or its close mouse homologue ERAAP was shown to affect cell-surface MHC-I levels and to specifically enhance MHC-I levels in baseline cell culture but to reduce MHC-I levels in cells treated with interferon-gamma (a cytokine known to enhance overall antigen presentation by increasing the expression of several proteins in the antigen presentation pathway, including ERAP1 [18, 54, 69]). These and subsequent studies suggested that ERAP1 can either destroy or generate peptide cargo for MHC-I, depending on other factors, including its own expression levels, MHC-I expression levels, availability of peptides in the ER, and peptide sequence. Further studies have validated this initial notion and have highlighted ERAP1 as an MHC-I cargo editor [20, 73]. The results presented here on the effects of pharmacological inhibition of ERAP1 on the immunopeptidome of melanoma cells are consistent with this notion. Chemical inhibition of ERAP1 shifts part of the immunopeptidome without abrogating overall MHC-I presentation. It is, however, surprising that in our model system ERAP1 inhibition appears to induce the presentation of many MHC-I-optimized peptides, consistent with a baseline destructive role of ERAP1. This finding, however, does correlate with a proposed role of ERAP1 in tumor cell immune evasion: ERAP1 can be up-regulated [37] to destroy tumor-specific antigens to facilitate immune evasion of $CD8^+$- or NK-mediated cytotoxic responses. Specifically for melanoma, recent work has shown that ERAP1 can destroy a potent tumor-associated antigenic peptide and ERAP1 down-regulation can enhance anti-tumor cytotoxicity and anti-PD-1 immunotherapy [10, 39]. Our work here suggests that chemical inhibition of ERAP1 can affect the presentation of hundreds to thousands of peptides, effectively inducing antigenic shifts that increase the chances that an immune-evading tumor will be recognized by the immune system.

Studies on the immunopeptidome of other cell lines and transgenic animals

The effects of ERAP1 on the immunopeptidome have been studied in several human cell lines [34, 50, 74]. In those studies, the authors compared the immunopeptidome presented by particular HLA alleles (namely HLA-B*27, HLA-A*29:02, HLA-B*51) from cell lines expressing alleles of ERAP1 that have different activity and selectivity [32, 35]. Detailed proteomic analysis demonstrated effects of differential ERAP1 activity on antigen presentation and supported the role of ERAP1 haplotypes on HLA-associated inflammatory autoimmunity (reviewed in [27]). Overall, these previous studies had suggested that ERAP1 affects a fraction of the peptidome and that its down-regulation can lead to increased frequency of longer peptides and can affect the nature of the first amino acid, all effects consistent with a productive role of ERAP1. Significant knowledge on the biology of ERAP1 has been derived from animal studies. Most of those studies have focused on the effect of ERAP1 knockout ($eraap^{-/-}$) on immunodominance and immunogenicity, and have described strong, albeit variable, effects on both these areas [19, 20, 24]. Two recent studies have performed deep proteomic analysis of the effects of ERAP1 deletion on knockout animals. In one study, the authors analyzed the peptidome of HLA-B27 transgenic rats and found that ERAP1 deletion affected only a subset of the peptidome with additional effects on peptide length and sequence [25]. In another study, the authors analyzed the effects of ERAP1 deletion on the immunopeptidome of bone marrow-derived

dendritic cells of transgenic mice, and described strong shifts in both sequence and length [57]. Overall the effects of the ERAP1 inhibitor on the melanoma cell line described here are consistent with the effects described in other cell lines and transgenic/knockout animals—namely changes restricted to a subset of the peptidome, including effects on peptide length and sequence. It is notable, however, that in our system, chemical ERAP1 inhibition also appears to eradicate a subset of elongated peptides with poor affinity for MHC-I that are resistant to ERAP1 trimming primarily due to the presence of a Pro residue at position 1 or 2 of the sequence. Furthermore, ERAP1 inhibition leads to the generation of hundreds of new and affinity-optimized MHC-I ligands that include peptides between 10–12 amino acids long that potentially can be immunogenic. This phenomenon is consistent with a baseline destructive effect of ERAP1 in this cell line and fits well with previous observations that ERAP1 can destroy an immunogenic epitope in another melanoma cell line [39], and that its activity can promote immune evasion [28, 37]. While this effect may be cell line specific, it provides support to the hypothesis that ERAP1 inhibition in cancer may promote immunogenicity [75].

Chemical versus genetic down-regulation of ERAP1 activity

An additional issue to consider when comparing genetic to pharmacological approaches, especially in the context of antigen processing and presentation, is the kinetics of the system. Antigen processing and presentation is a highly dynamic competitive system in which many different antigens compete for few positions on the MHC at the cell surface. Short-term chemical inhibition may not be able to fully reproduce permanent genetic changes in cells due to this kinetic component. Furthermore, all inhibitors, regardless of their known specificity, may have off-target effects, which, even if they are outside the biochemical pathway targeted, may still affect antigen presentation by altering the cellular proteome. Regardless of this complication, evaluating the effects of ERAP1 inhibition by chemical compounds is a prerequisite to any pre-clinical development of compounds with pharmaceutical interest and central to the development of therapeutic applications. Furthermore, in vivo genetic down-regulation model systems (i.e. ,knockout animals) may be of limited value in predicting the effects of chemical inhibition for at least two main reasons: i) differences in the gene components of the pathway between humans and experimental animals, which are quite common for components of immune system pathways, and ii) modifications and adjustments of the cellular proteome and presentation during the generation of tolerance and among different cell lines. Regardless of these limitations, treating the A375 melanoma cell line with the DG013A inhibitor does appear to reproduce the effects that would be expected from ERAP1 activity down-regulation, and supports the main hypothesis that using an ERAP1 inhibitor is a valid approach for manipulating the immunopeptidome of cells without generating any major defects in the quality of antigen presentation.

Potential impact on anti-cancer responses: limitations of the study

While the results described in this study hint to possible alterations of the immunogenicity of melanoma upon treatment with the inhibitor in vivo, key limitations of the scope of this study need to be acknowledged to avoid overinterpretation. Indeed, the finding that the inhibitor induces the presentation of many new MHC-I presented peptides could raise hopes regarding the therapeutic potential of this approach in enhancing the immunogenicity of cancer. However, this would be speculative at this point since immunogenicity and anti-tumor responses were not examined. Furthermore, potential off-target and off-function side effects could complicate interpretation of results as well as therapeutic applications. Indeed, DG013A is not selective versus the highly homologous enzyme ERAP2, which, however, has more limited effects in antigen presentation and is poorly expressed in A375 cells. Regardless, the lack of selectivity of DG013A versus homologous aminopeptidases is a limiting factor for clinical development. Furthermore, ERAP1 has been reported to have other functions that could complicate therapeutic approaches and are not examined here (reviewed in [76]). More specifically, reports have demonstrated ERAP1 involvement in other aspects of the immune response, in particular cytokine receptor shedding and macrophage activation [77, 78]. Additionally, although inhibitor treatment generated novel MHC-I ligands, it also abrogated many, suggesting that it could be detrimental to some existing anti-tumor immune responses. Given, however, that most cancers develop immune evasion [79], the generation of novel antigenic peptides may outweigh the destruction of some existing ones. Further studies are necessary to address these potential caveats and to explore in more detail the global effects of ERAP1 inhibition on the immune system.

Although ERAP1 inhibition may bring about desirable shifts in the immunopeptidome of cancer cells, systemic delivery will likely induce immunopeptidome shifts in normal cells as well, raising concerns that about induction of autoimmune-like responses. While these effects certainly are undesirable, they may be tolerable, not unlike the situation with immune-checkpoint inhibitor therapy approaches that can also target normal cells and present serious side effects, yet are successful clinically. Immunogenicity requires the coordination of several signals, of which antigen presentation is only one. As a result, reprogramming antigen

presentation may shift the balance towards new immune responses only in systems that are immunogenic to begin with. Indeed, it has been shown previously that cytomegalovirus induces infected cells to down-regulate ERAP1 expression via a particular microRNA as part at its immune evasion strategy [36]. While these infections are common in the population, no association between human CMV infection and autoimmunity has been demonstrated, an observation that suggests that lowering ERAP1 activity could have a rather minor effect on the immunogenicity of healthy cells.

Pharmacological applications for enhancing immunogenicity of cancer

In summary, we present here a detailed HLA peptidomics analysis of how the immunopeptidome of the A375 melanoma cell line is regulated by a potent ERAP1 inhibitor. We find that the inhibitor affects about half of the immunopeptidome and a third of the good MHC-I ligands, and induces the presentation of many peptides that are predicted to be optimal ligands for MHC-I. Our results suggest significant target engagement by the inhibitor and are consistent with the known biology of ERAP1 as accumulated by genetic down-regulation and functional studies. However, our results also highlight some key differences from previous studies, which may be the result of the transient nature of the inhibition or from off-target effects that need to be further evaluated. This is the first study, to our knowledge, that has explored the use of a particular inhibitor to induce short-term ERAP1-dependent immunopeptidome shifts. Furthermore, our results suggest that ERAP1 activity in melanoma is important for shaping a part of the final MHC-I peptide repertoire and may be exploitable for enhancing immunogenicity. Given the current interest in enhancing tumor antigenicity for cancer immunotherapy, our results provide experimental support that ERAP1 inhibition can constitute a promising approach towards that goal. This may be especially true for supplementing immune-checkpoint inhibitor immunotherapy as recently demonstrated in a melanoma mouse tumor model in which genetic ERAP1 depletion increased the efficacy of anti-PD-1 immunotherapy [10]. Future studies will undoubtedly have to focus on exploring the applicability of these pharmacologically induced immunopeptidome shifts to enhancing anti-cancer or suppressing auto-inflammatory immune responses in relevant ex vivo or animal models.

Data deposition

The mass spectrometry data have been deposited to the ProteomeXchange Consortium via the PRIDE partner repository with the dataset identifier PXD011766. A MaxQuant style table listing all identified peptides and relevant parameters can be downloaded at https://sfiler.ipta.demokritos.gr/s/qMJGBCCE6oSqi5p using as password erap1a375.

Acknowledgements The authors are also grateful to Kenneth Rock for providing the HeLa-Kb cells and recombinant vaccinia, and to Lianjun Shen for technical advice on optimizing the cellular antigen processing assay.

Author contributions Despoina Koumantou designed, performed cellular and proteomic experiments and analyzed data with assistance from Adrian Martin-Esteban. Eilon Barnea and Arie Admon performed the proteomics analysis and analyzed and interpreted data. Anastasia Mpakali assisted with the characterization of A375 cells. Harris Pratsinis helped with the FACS analysis. Paraskevi Kokkala and Dimitris Georgiadis synthesized the ERAP1 inhibitor. Athanasios Papakyriakou performed the analysis for neoantigen-derived peptides. Zachary Maben performed cellular inhibitor studies. Lawrence J. Stern supervised the presentation assay and analyzed data. Efstratios Stratikos supervised the project, analyzed data and prepared the manuscript with input from all authors. All authors have approved the manuscript's final version.

Funding This research was funded by the Harry J. Lloyd Charitable Trust through a grant to Efstratios Stratikos. The authors also acknowledge financial support by the project "NCSRD—INRASTES research activities in the framework of the national RIS3." (MIS 5002559) which is implemented under the "Action for the Strategic Development on the Research and Technological Sector", funded by the Operational Programme "Competitiveness, Entrepreneurship and Innovation" (NSRF 2014-2020) and co-financed by Greece and the European Union (European Regional Development Fund). The authors would also like to acknowledge funding from the National Institutes of Health (Grants AI038996 and AI137198 to Lawrence J. Stern) and funding by the Israel Science Foundation (Grant no. 534165 to Arie Admon). Adrian Martin-Esteban acknowledges financial support from the European Federation of Immunological Societies.

Compliance with ethical standards

Conflict of interest The authors declare they have no conflicts of interest.

Ethical approval The work described in this paper was performed using commercially available cell lines. Therefore, no study approval was required, and no informed consent from the donors.

Cell line authentication The A375 human malignant melanoma cell line and the W6/32 hybridoma cell line (CRL-1619 and HB-95, respectively) were purchased from American Type Culture Collection (ATCC) and used as provided by the vendor without any further authentication. The Hi5 insect cell line was purchased from Thermo Fischer Scientific and used as provided by the vendor without any further authentication. HeLa-Kb cells were provided by Kenneth Rock (University of Massachusetts Medical School, Worcester, MA, USA) and have been described before [18]. The expression of the MHC-I allele Kb by the HeLa-Kb cell line was confirmed by FACS staining.

References

1. Sharma P, Allison JP (2015) Immune checkpoint targeting in cancer therapy: toward combination strategies with

curative potential. Cell 161:205–214. https://doi.org/10.1016/j.cell.2015.03.030
2. Van Allen EM, Miao D, Schilling B et al (2015) Genomic correlates of response to CTLA-4 blockade in metastatic melanoma. Science 350:207–211. https://doi.org/10.1126/science.aad0095
3. Rizvi NA, Hellmann MD, Snyder A et al (2015) Cancer immunology. Mutational landscape determines sensitivity to PD-1 blockade in non-small cell lung cancer. Science 348:124–128. https://doi.org/10.1126/science.aaa1348
4. Balachandran VP, Luksza M, Zhao JN et al (2017) Identification of unique neoantigen qualities in long-term survivors of pancreatic cancer. Nature 551:512–516. https://doi.org/10.1038/nature24462
5. Schreiber RD, Old LJ, Smyth MJ (2011) Cancer immunoediting: integrating immunity's roles in cancer suppression and promotion. Science 331:1565–1570. https://doi.org/10.1126/science.1203486
6. Topalian SL, Drake CG, Pardoll DM (2015) Immune checkpoint blockade: a common denominator approach to cancer therapy. Cancer Cell 27:450–461. https://doi.org/10.1016/j.ccell.2015.03.001
7. Bukur J, Jasinski S, Seliger B (2012) The role of classical and non-classical HLA class I antigens in human tumors. Semin Cancer Biol 22:350–358. https://doi.org/10.1016/j.semcancer.2012.03.003
8. Kamphorst AO, Wieland A, Nasti T et al (2017) Rescue of exhausted CD8 T cells by PD-1-targeted therapies is CD28-dependent. Science 355:1423–1427. https://doi.org/10.1126/science.aaf0683
9. Hui E, Cheung J, Zhu J et al (2017) T cell costimulatory receptor CD28 is a primary target for PD-1-mediated inhibition. Science 355:1428–1433. https://doi.org/10.1126/science.aaf1292
10. Manguso RT, Pope HW, Zimmer MD et al (2017) In vivo CRISPR screening identifies Ptpn2 as a cancer immunotherapy target. Nature 547:413–418. https://doi.org/10.1038/nature23270
11. Tran E, Ahmadzadeh M, Lu YC et al (2015) Immunogenicity of somatic mutations in human gastrointestinal cancers. Science 350:1387–1390. https://doi.org/10.1126/science.aad1253
12. Weimershaus M, Evnouchidou I, Saveanu L, van Endert P (2013) Peptidases trimming MHC class I ligands. Curr Opin Immunol 25:90–96. https://doi.org/10.1016/j.coi.2012.10.001
13. Evnouchidou I, Papakyriakou A, Stratikos E (2009) A new role for Zn(II) aminopeptidases: antigenic peptide generation and destruction. Curr Pharm Des 15:3656–3670
14. de Castro JAL (2018) How ERAP1 and ERAP2 shape the peptidomes of disease-associated MHC-I proteins. Front Immunol. https://doi.org/10.3389/fimmu.2018.02463
15. Stratikos E, Stern LJ (2013) Antigenic peptide trimming by ER aminopeptidases—insights from structural studies. Mol Immunol 55:212–219. https://doi.org/10.1016/j.molimm.2013.03.002
16. Alvarez-Navarro C, Lopez de Castro JA (2014) ERAP1 structure, function and pathogenetic role in ankylosing spondylitis and other MHC-associated diseases. Mol Immunol 57:12–21. https://doi.org/10.1016/j.molimm.2013.06.012
17. Saveanu L, Carroll O, Lindo V et al (2005) Concerted peptide trimming by human ERAP1 and ERAP2 aminopeptidase complexes in the endoplasmic reticulum. Nat Immunol 6:689–697. https://doi.org/10.1038/ni1208
18. York IA, Chang SC, Saric T, Keys JA, Favreau JM, Goldberg AL, Rock KL (2002) The ER aminopeptidase ERAP1 enhances or limits antigen presentation by trimming epitopes to 8–9 residues. Nat Immunol 3:1177–1184
19. York IA, Brehm MA, Zendzian S, Towne CF, Rock KL (2006) Endoplasmic reticulum aminopeptidase 1 (ERAP1) trims MHC class I-presented peptides in vivo and plays an important role in immunodominance. Proc Natl Acad Sci USA 103:9202–9207
20. Hammer GE, Gonzalez F, James E, Nolla H, Shastri N (2007) In the absence of aminopeptidase ERAAP, MHC class I molecules present many unstable and highly immunogenic peptides. Nat Immunol 8:101–108
21. Cifaldi L, Lo Monaco E, Forloni M et al (2011) Natural killer cells efficiently reject lymphoma silenced for the endoplasmic reticulum aminopeptidase associated with antigen processing. Cancer Res 71:1597–1606. https://doi.org/10.1158/0008-5472.CAN-10-3326
22. James E, Bailey I, Sugiyarto G, Elliott T (2013) Induction of Protective Antitumor Immunity through Attenuation of ERAAP Function. J. Immunol. 190:5839–5846. https://doi.org/10.4049/jimmunol.1300220
23. Nagarajan NA, Gonzalez F, Shastri N (2012) Nonclassical MHC class Ib-restricted cytotoxic T cells monitor antigen processing in the endoplasmic reticulum. Nat Immunol 13:579–586. https://doi.org/10.1038/ni.2282
24. Rastall DP, Aldhamen YA, Seregin SS, Godbehere S, Amalfitano A (2014) ERAP1 functions override the intrinsic selection of specific antigens as immunodominant peptides, thereby altering the potency of antigen-specific cytolytic and effector memory T-cell responses. Int Immunol 26:685–695. https://doi.org/10.1093/intimm/dxu078
25. Barnea E, Melamed Kadosh D, Haimovich Y et al (2017) The human leukocyte antigen (HLA)-B27 peptidome in vivo, in spondyloarthritis-susceptible HLA-B27 transgenic rats and the effect of Erap1 deletion. Mol Cell Proteomics 16:642–662. https://doi.org/10.1074/mcp.M116.066241
26. Georgiadou D, Stratikos E (2009) Cellular mechanisms that edit the immunopeptidome. Curr Proteomics 6:13–24
27. Lopez de Castro JA, Alvarez-Navarro C, Brito A, Guasp P, Martin-Esteban A, Sanz-Bravo A (2016) Molecular and pathogenic effects of endoplasmic reticulum aminopeptidases ERAP1 and ERAP2 in MHC-I-associated inflammatory disorders: towards a unifying view. Mol Immunol 77:193–204. https://doi.org/10.1016/j.molimm.2016.08.005
28. Stratikos E, Stamogiannos A, Zervoudi E, Fruci D (2014) A role for naturally occurring alleles of endoplasmic reticulum aminopeptidases in tumor immunity and cancer pre-disposition. Front Oncol. 4:363. https://doi.org/10.3389/fonc.2014.00363
29. Cortes A, Pulit SL, Leo PJ et al (2015) Major histocompatibility complex associations of ankylosing spondylitis are complex and involve further epistasis with ERAP1. Nat Commun 6:7146. https://doi.org/10.1038/ncomms8146
30. The Australo-Anglo-American Spondyloarthritis C, the Wellcome Trust Case Control C, Evans DM et al (2011) Interaction between ERAP1 and HLA-B27 in ankylosing spondylitis implicates peptide handling in the mechanism for HLA-B27 in disease susceptibility. Nat Genet 43:761–767. https://doi.org/10.1038/ng.873
31. Mehta AM, Jordanova ES, Corver WE, van Wezel T, Uh HW, Kenter GG, Jan Fleuren G (2009) Single nucleotide polymorphisms in antigen processing machinery component ERAP1 significantly associate with clinical outcome in cervical carcinoma. Genes Chromosom Cancer 48:410–418
32. Evnouchidou I, Kamal RP, Seregin SS et al (2011) Coding single nucleotide polymorphisms of endoplasmic reticulum aminopeptidase 1 can affect antigenic peptide generation in vitro by influencing basic enzymatic properties of the enzyme. J. Immunol. 186:1909–1913. https://doi.org/10.4049/jimmunol.1003337
33. Reeves E, Colebatch-Bourn A, Elliott T, Edwards CJ, James E (2014) Functionally distinct ERAP1 allotype combinations distinguish individuals with Ankylosing Spondylitis. Proc Natl Acad Sci USA 111:17594–17599. https://doi.org/10.1073/pnas.1408882111
34. Sanz-Bravo A, Campos J, Mazariegos MS, Lopez de Castro JA (2015) Dominant role of the ERAP1 polymorphism R528K in

shaping the HLA-B27 peptidome through differential processing determined by multiple peptide residues. Arthritis Rheumatol 67:692–701. https://doi.org/10.1002/art.38980
35. Reeves E, Edwards CJ, Elliott T, James E (2013) Naturally occurring ERAP1 haplotypes encode functionally distinct alleles with fine substrate specificity. J Immunol 191:35–43. https://doi.org/10.4049/jimmunol.1300598
36. Kim S, Lee S, Shin J et al (2011) Human cytomegalovirus microRNA miR-US4-1 inhibits CD8(+) T cell responses by targeting the aminopeptidase ERAP1. Nat Immunol 12:984–991. https://doi.org/10.1038/ni.2097
37. Fruci D, Giacomini P, Nicotra MR, Forloni M, Fraioli R, Saveanu L, van Endert P, Natali PG (2008) Altered expression of endoplasmic reticulum aminopeptidases ERAP1 and ERAP2 in transformed non-lymphoid human tissues. J Cell Physiol 216:742–749
38. Fruci D, Ferracuti S, Limongi MZ et al (2006) Expression of endoplasmic reticulum aminopeptidases in EBV-B cell lines from healthy donors and in leukemia/lymphoma, carcinoma, and melanoma cell lines. J. Immunol. 176:4869–4879
39. Keller M, Ebstein F, Burger E et al (2015) The proteasome immunosubunits, PA28 and ER-aminopeptidase 1 protect melanoma cells from efficient MART-126-35 -specific T-cell recognition. Eur J Immunol 45:3257–3268. https://doi.org/10.1002/eji.201445243
40. Chen L, Fischer R, Peng Y et al (2014) Critical role of endoplasmic reticulum aminopeptidase 1 in determining the length and sequence of peptides bound and presented by HLA-B27. Arthritis Rheumatol 66:284–294. https://doi.org/10.1002/art.38249
41. Cifaldi L, Romania P, Falco M et al (2015) ERAP1 regulates natural killer cell function by controlling the engagement of inhibitory receptors. Cancer Res 75:824–834. https://doi.org/10.1158/0008-5472.CAN-14-1643
42. Stratikos E (2014) Regulating adaptive immune responses using small molecule modulators of aminopeptidases that process antigenic peptides. Curr Opin Chem Biol 23C:1–7. https://doi.org/10.1016/j.cbpa.2014.08.007
43. Zervoudi E, Saridakis E, Birtley JR et al (2013) Rationally designed inhibitor targeting antigen-trimming aminopeptidases enhances antigen presentation and cytotoxic T-cell responses. Proc Natl Acad Sci USA 110:19890–19895. https://doi.org/10.1073/pnas.1309781110
44. Aldhamen YA, Pepelyayeva Y, Rastall DP et al (2015) Autoimmune disease-associated variants of extracellular endoplasmic reticulum aminopeptidase 1 induce altered innate immune responses by human immune cells. J Innate Immun 7:275–289. https://doi.org/10.1159/000368899
45. Chen L, Ridley A, Hammitzsch A, Al-Mossawi MH, Bunting H, Georgiadis D, Chan A, Kollnberger S, Bowness P (2016) Silencing or inhibition of endoplasmic reticulum aminopeptidase 1 (ERAP1) suppresses free heavy chain expression and Th17 responses in ankylosing spondylitis. Ann Rheum Dis 75:916–923. https://doi.org/10.1136/annrheumdis-2014-206996
46. Zervoudi E, Papakyriakou A, Georgiadou D et al (2011) Probing the S1 specificity pocket of the aminopeptidases that generate antigenic peptides. Biochem J 435:411–420. https://doi.org/10.1042/BJ20102049
47. Kokkala P, Mpakali A, Mauvais FX et al (2016) Optimization and structure–activity relationships of phosphinic pseudotripeptide inhibitors of aminopeptidases that generate antigenic peptides. J Med Chem 59:9107–9123. https://doi.org/10.1021/acs.jmedchem.6b01031
48. Chen H, Noble F, Mothe A, Meudal H, Coric P, Danascimento S, Roques BP, George P, Fournie-Zaluski MC (2000) Phosphinic derivatives as new dual enkephalin-degrading enzyme inhibitors: synthesis, biological properties, and antinociceptive activities. J Med Chem 43:1398–1408. https://doi.org/10.1021/jm990483l
49. Makaritis A, Georgiadis D, Dive V, Yiotakis A (2003) Diastereoselective solution and multipin-based combinatorial array synthesis of a novel class of potent phosphinic metalloprotease inhibitors. Chemistry 9:2079–2094. https://doi.org/10.1002/chem.200204456
50. Guasp P, Barnea E, Gonzalez-Escribano MF, Jimenez-Reinoso A, Regueiro JR, Admon A, Lopez de Castro JA (2017) The Behcet's disease-associated variant of the aminopeptidase ERAP1 shapes a low-affinity HLA-B*51 peptidome by differential subpeptidome processing. J Biol Chem 292:9680–9689. https://doi.org/10.1074/jbc.M117.789180
51. Cox J, Mann M (2008) MaxQuant enables high peptide identification rates, individualized p.p.b.-range mass accuracies and proteome-wide protein quantification. Nat Biotechnol 26:1367–1372. https://doi.org/10.1038/nbt.1511
52. Porgador A, Yewdell JW, Deng Y, Bennink JR, Germain RN (1997) Localization, quantitation, and in situ detection of specific peptide-MHC class I complexes using a monoclonal antibody. Immunity 6:715–726
53. Schuler MM, Nastke MD, Stevanovikc S (2007) SYFPEITHI: database for searching and T-cell epitope prediction. Methods Mol Biol 409:75–93
54. Saric T, Chang SC, Hattori A, York IA, Markant S, Rock KL, Tsujimoto M, Goldberg AL (2002) An IFN-gamma-induced aminopeptidase in the ER, ERAP1, trims precursors to MHC class I-presented peptides. Nat Immunol 3:1169–1176
55. Petryszak R, Keays M, Tang YA et al (2016) Expression Atlas update—an integrated database of gene and protein expression in humans, animals and plants. Nucleic Acids Res 44:D746–D752. https://doi.org/10.1093/nar/gkv1045
56. Ombrello MJ, Kastner DL, Remmers EF (2015) Endoplasmic reticulum-associated amino-peptidase 1 and rheumatic disease: genetics. Curr Opin Rheumatol 27:349–356. https://doi.org/10.1097/BOR.0000000000000189
57. Nagarajan NA, de Verteuil DA, Sriranganadane D, Yahyaoui W, Thibault P, Perreault C, Shastri N (2016) ERAAP shapes the peptidome associated with classical and nonclassical MHC class I molecules. J Immunol 197:1035–1043. https://doi.org/10.4049/jimmunol.1500654
58. Assarsson E, Sidney J, Oseroff C et al (2007) A quantitative analysis of the variables affecting the repertoire of T cell specificities recognized after vaccinia virus infection. J Immunol 178:7890–7901
59. Sette A, Vitiello A, Reherman B et al (1994) The relationship between class I binding affinity and immunogenicity of potential cytotoxic T cell epitopes. J Immunol 153:5586–5592
60. Karosiene E, Lundegaard C, Lund O, Nielsen M (2012) NetMHCcons: a consensus method for the major histocompatibility complex class I predictions. Immunogenetics 64:177–186. https://doi.org/10.1007/s00251-011-0579-8
61. Cancer Cell Line Encyclopedia C, Genomics of Drug Sensitivity in Cancer C (2015) Pharmacogenomic agreement between two cancer cell line data sets. Nature 528:84–87. https://doi.org/10.1038/nature15736
62. Abelin JG, Keskin DB, Sarkizova S et al (2017) Mass spectrometry profiling of HLA-associated peptidomes in mono-allelic cells enables more accurate epitope prediction. Immunity 46:315–326. https://doi.org/10.1016/j.immuni.2017.02.007
63. Mpakali A, Maben Z, Stern LJ, Stratikos E (2018) Molecular pathways for antigenic peptide generation by ER aminopeptidase 1. Immunol, Mol. https://doi.org/10.1016/j.molimm.2018.03.026
64. Hearn A, York IA, Rock KL (2009) The specificity of trimming of MHC class I-presented peptides in the endoplasmic reticulum. J. Immunol. 183:5526–5536
65. Landon M (1977) Cleavage at aspartyl-prolyl bonds. Methods Enzymol 47:145–149

66. Andreatta M, Alvarez B, Nielsen M (2017) GibbsCluster: unsupervised clustering and alignment of peptide sequences. Nucleic Acids Res 45:W458–W463. https://doi.org/10.1093/nar/gkx248
67. Thomsen MC, Nielsen M (2012) Seq2Logo: a method for construction and visualization of amino acid binding motifs and sequence profiles including sequence weighting, pseudo counts and two-sided representation of amino acid enrichment and depletion. Nucleic Acids Res 40:W281–W287. https://doi.org/10.1093/nar/gks469
68. Andreatta M, Lund O, Nielsen M (2013) Simultaneous alignment and clustering of peptide data using a Gibbs sampling approach. Bioinformatics 29:8–14. https://doi.org/10.1093/bioinformatics/bts621
69. Serwold T, Gonzalez F, Kim J, Jacob R, Shastri N (2002) ERAAP customizes peptides for MHC class I molecules in the endoplasmic reticulum. Nature 419:480–483
70. Komov L, Kadosh DM, Barnea E, Milner E, Hendler A, Admon A (2018) Cell Surface MHC class i expression is limited by the availability of peptide-receptive "empty" molecules rather than by the supply of peptide ligands. Proteomics 18:e1700248. https://doi.org/10.1002/pmic.201700248
71. Paulson KG, Tegeder A, Willmes C et al (2014) Downregulation of MHC-I expression is prevalent but reversible in Merkel cell carcinoma. Cancer Immunol Res 2:1071–1079. https://doi.org/10.1158/2326-6066.CIR-14-0005
72. Boegel S, Lower M, Bukur T, Sahin U, Castle JC (2014) A catalog of HLA type, HLA expression, and neo-epitope candidates in human cancer cell lines. Oncoimmunology 3:e954893. https://doi.org/10.4161/21624011.2014.954893
73. Hammer GE, Kanaseki T, Shastri N (2007) The final touches make perfect the peptide-MHC class I repertoire. Immunity 26:397–406. https://doi.org/10.1016/j.immuni.2007.04.003
74. Martin-Esteban A, Sanz-Bravo A, Guasp P, Barnea E, Admon A, Lopez de Castro JA (2017) Separate effects of the ankylosing spondylitis associated ERAP1 and ERAP2 aminopeptidases determine the influence of their combined phenotype on the HLA-B*27 peptidome. J Autoimmun 79:28–38. https://doi.org/10.1016/j.jaut.2016.12.008
75. Stratikos E (2014) Modulating antigen processing for cancer immunotherapy. Oncoimmunology 3:e27568. https://doi.org/10.4161/onci.27568
76. Georgiadis D, Mpakali A, Koumantou D, Stratikos E (2018) Inhibitors of ER aminopeptidase 1 and 2: from design to clinical application. Curr Med Chem 1:10. https://doi.org/10.2174/0929867325666180214111849
77. Cui X, Rouhani FN, Hawari F, Levine SJ (2003) Shedding of the type II IL-1 decoy receptor requires a multifunctional aminopeptidase, aminopeptidase regulator of TNF receptor type 1 shedding. J Immunol 171:6814–6819
78. Goto Y, Ogawa K, Hattori A, Tsujimoto M (2011) Secretion of endoplasmic reticulum aminopeptidase 1 is involved in the activation of macrophages induced by lipopolysaccharide and interferon-gamma. J Biol Chem 286:21906–21914. https://doi.org/10.1074/jbc.m111.239111
79. Dunn GP, Old LJ, Schreiber RD (2004) The three Es of cancer immunoediting. Annu Rev Immunol 22:329–360. https://doi.org/10.1146/annurev.immunol.22.012703.104803